The American Journal of Pathology, Vol. 192, No. 8, August 2022

ELSEVIER

The American Journal of PATHOLOGY

ajp.amjpathol.org

CARDIOVASCULAR, PULMONARY, AND RENAL PATHOLOGY

A Morphomolecular Approach to Alveolar Capillary Dysplasia

Jan C. Kamp,[*†] Lavinia Neubert,[†‡] Maximilian Ackermann,[§¶] Helge Stark,[†‡] Edith Plucinski,[†‡] Harshit R. Shah,[†‡] Sabina Janciauskiene,[*†] Anke K. Bergmann,[‖] Gunnar Schmidt,[‖] Tobias Welte,[*†] Axel Haverich,[†**] Christopher Werlein,[†‡] Peter Braubach,[†‡] Florian Laenger,[†‡] Nicolaus Schwerk,[††] Karen M. Olsson,[*†] Jan Fuge,[*†] Da-Hee Park,[*†] Jonas C. Schupp,[*†] Marius M. Hoeper,[*†] Mark P. Kuehnel,[†‡] and Danny D. Jonigk[†‡]

From the Departments of Respiratory Medicine and Cardiothoracic, Transplant and Vascular Surgery,** the Institute of Pathology,[‡] the Institute of Human Genetics,[‖] and the Clinic for Pediatric Pneumology, Allergology, and Neonatology,[††] Hannover Medical School, Hannover; Biomedical Research in Endstage and Obstructive Lung Disease Hannover,[†] German Center for Lung Research, Hannover; the Institute of Functional and Clinical Anatomy,[§] University Medical Center of the Johannes Gutenberg—University Mainz, Mainz, Germany, and the Institute of Pathology and Department of Molecular Pathology,[¶] Helios University Clinic Wuppertal, University of Witten—Herdecke, Wuppertal, Germany*

Accepted for publication May 11, 2022.

Address correspondence to Jan C. Kamp, M.D., Department of Respiratory Medicine, Hannover Medical School, Carl-Neuberg-Str. 1, 30625 Hannover, Germany.
E-mail: kamp.jan-christopher@mh-hannover.de.

Alveolar capillary dysplasia (ACD) is a rare lung developmental disorder leading to persistent pulmonary arterial hypertension and fatal outcomes in newborns. The current study analyzed the microvascular morphology and the underlying molecular background of ACD. One ACD group ($n = 7$), one pulmonary arterial hypertension group ($n = 20$), and one healthy con1trol group ($n = 16$) were generated. Samples of histologically confirmed ACD were examined by exome sequencing and array-based comparative genomic hybridization. Vascular morphology was analyzed using scanning electron microscopy of microvascular corrosion casts. Gene expression and biological pathways were analyzed using two panels on inflammation/kinase-specific genes and a comparison analysis tool. Compartment-specific protein expression was analyzed using immunostaining. In ACD, there was an altered capillary network, a high prevalence of intussusceptive angiogenesis, and increased activity of C-X-C motif chemokine receptor 4 (CXCR4), hypoxia-inducible factor 1α (HIF1A), and angiopoietin signaling pathways compared with pulmonary arterial hypertension/healthy controls. Histologically, there was a markedly increased prevalence of endothelial tyrosine kinase receptor (TEK/TIE2)$^+$ macrophages in ACD, compared with the other groups, whereas the CXCR4 ligand CXCL12 and HIF1A showed high expression in all groups. ACD is characterized by dysfunctional capillaries and a high prevalence of intussusceptive angiogenesis. The results indicate that endothelial CXCR4, HIF1A, and angiopoietin signaling as well as TIE2$^+$ macrophages are crucial for the induction of intussusceptive angiogenesis and vascular remodeling. Future studies should address the use of anti-angiogenic agents in ACD, where TIE2 appears as a promising target. *(Am J Pathol 2022, 192: 1110—1121; https://doi.org/10.1016/j.ajpath.2022.05.004)*

Persistent pulmonary hypertension of the newborn is a rare clinical condition resulting from the failed transition from *in utero* to post-partum circulation, with an annual incidence rate of 30.1 cases per million children.[1] The fetal circulation is characterized by high pulmonary vascular resistance and low pulmonary blood flow.[2] Physiologically, this constellation

Supported by PRACTIS—Clinician Scientist Program of Hannover Medical School, funded by the German Research Foundation ME 3696/3-1 and KFO311-286251789 (J.C.K.); the European Research Council grant (D.D.J.); and the European Consolidator grant, XHaLe (reference number 771883).

J.C.K. and L.N. contributed equally to this work.

M.P.K. and D.D.J. contributed equally to this work as senior authors.

Disclosures: J.C.K., L.N., M.A., H.S., E.P., H.R.S., S.J., A.K.B., G.S., T.W., A.H., C.W., P.B., F.L., N.S., J.F., J.C.S., M.P.K., and D.D.J. declare that they have no conflicts of interest. M.M.H. has received fees for lectures and/or consultations from Acceleron, Actelion, Bayer, GSK, Janssen, MSD, and Pfizer; K.M.O. has received fees for lectures and/or consultations from Acceleron, Actelion, Bayer, GSK, Janssen, MSD, Pfizer, and United Therapeutics; D.-H.P. has received fees for lectures and/or consultations from Janssen.

https://doi.org/10.1016/j.ajpath.2022.05.004

reverses within minutes after delivery with a decrease in pulmonary vascular resistance and increased pulmonary blood flow. Failure of this circulatory adaptation results in persistent pulmonary hypertension of the newborn, which, in turn, leads to right-to-left shunting of blood through the patent ductus arteriosus or the foramen ovale and causes severe hypoxemia.[3]

Alveolar capillary dysplasia (ACD) is a rare underlying disease of persistent pulmonary hypertension of the newborn which frequently manifests concomitantly with a suspected misalignment of the pulmonary veins (MPV).[4] In the current classification of children's interstitial lung diseases, ACD is assigned to group A2, related to lung developmental disorders.[5] Affected infants experience respiratory distress and cyanosis immediately or within the first weeks after birth,[6] whereas later presentations are less frequent.[7,8] In contrast to other severe children's interstitial lung disease entities manifesting during early infancy, such as surfactant-related disorders, the leading symptom is pulmonary hypertension, and radiological signs, such as diffuse ground glass opacities, are often missing. In most cases, ACD is a fatal developmental disorder of the pulmonary vasculature, and the only option for survival is lung transplantation, which is extremely challenging in newborns.[9,10]

To date, >200 ACD cases have been documented. Approximately 60% of all reported cases have been associated with distinct heterozygous variants of forkhead box F1 (*FOXF1*) gene (located at 16q24.1), its transcriptional enhancer (located 257 kb 5′ to *FOXF1*), or other genetic alterations.[11,12] Histopathologic features of ACD include the following: i) the presence of reduced and dysplastic alveoli; ii) a suspected MPV (ie, abnormal placement of pulmonary artery and vein in the same bronchiovascular bundle); iii) a rarefaction in pulmonary capillarization; iv) widened or thickened alveolar septa with concomitant apposition deficiency of the alveolar capillaries to the alveolar epithelia; v) medial hypertrophy of the small pulmonary arteries; vi) dilation of the pulmonary veins; and vii) incidence of thrombi in dilated veins or hypertrophied arteries.[13–15]

Data on the molecular mechanisms leading to ACD, as well as data on the origin of the misaligned pulmonary veins in ACD, are still limited and partially controversial. In a recent work, Norvik et al[16] analyzed the vascular microanatomy of ACD cases with suspected MPV using Synchrotron-based phase-contrast microcomputed X-ray tomography. They confirmed the existence of intrapulmonary bronchopulmonary shunts, which have previously also been reported by other groups.[13] In addition, they found suspected misaligned pulmonary veins in the designated position of bronchial veins/venules and hypothesized that these were not pulmonary, but bronchial, veins/venules. Recently, functional relevance of bronchopulmonary shunts for continued perfusion has been demonstrated in several other pulmonary diseases,[17] expanding the hypothesis by Norvik et al[16] to additional diseases.

This study further analyzed the vascular morphology of ACD and used molecular analyses to gain new insights into this rare but fatal disease.

Materials and Methods

Study Groups and Histopathology

As ACD represents one entity out of the spectrum of pulmonary hypertensive disease, three study groups were generated: one ACD group, one group of patients diagnosed with idiopathic pulmonary arterial hypertension (PAH), and one group of healthy controls. Of the ACD group, all samples were formalin fixed, paraffin embedded (FFPE) and come from infants with a diagnosis of ACD with or without MPV. Samples were collected in the period 2005 to 2020 and were taken from the archives of the Institute of Pathology at Hannover Medical School (Hannover, Germany) and retrospectively reviewed. For the PAH group, FFPE material was selected from $n = 20$ lung explants; and for the control group, FFPE material was used from human pulmonary down-sizing specimens from $n = 16$ donors (ie, healthy tissues from lung grafts that were oversized in regard to the recipients' thorax, and therefore, were surgically down sized during transplantation). Every sample that was used as a control was diagnosed as healthy via histopathologic assessment before sampling. Sagittal sections were taken bilaterally from all lung lobes. Approximately 1-μm thick sections were cut and stained with hematoxylin and eosin, periodic acid–Schiff, and elastic van Gieson dyes. Diagnosis of ACD required the presence of widened or thickened alveolar septa with concomitant apposition deficiency of the alveolar capillaries to the alveolar epithelia and rarefaction in pulmonary capillarization as well as signs of pulmonary arterial hypertension, such as medial hypertrophy of the small pulmonary arteries. Cases with and without MPV were differentiated according to the presence of suspected misaligned pulmonary veins within the bronchiovascular bundle. This study was approved by the local ethics committee at Hannover Medical School (ethics vote number 2702-2015). All subjects or their relatives gave written informed consent.

Genetic Analysis

DNA was isolated from FFPE blocks using the Maxwell RSC DNA FFPE Kit (Promega Corp., Madison, WI). DNA content was measured using the NanoDrop one microvolume UV-vis spectrophotometer (Thermo Fisher Scientific, Waltham, MA), guaranteeing a minimum of 500 ng DNA in each sample. Whole exome sequencing and array-based comparative genomic hybridization were performed to analyze genetic variants that have been suggested to play a role in ACD in former studies to better characterize the study group. Genes analyzed were dedicator of cytokinesis 8 (*DOCK8*), epithelial splicing regulatory protein 1

(*ESRP1*), *FOXF1*, myosin phosphatase rho-interacting protein (*MPRIP*), plexin B2 (*PLXNB2*), solute carrier family 50 member 1 (*SLC50A1*), zinc finger myeloid, nervy, and deaf-type containing 11 (*ZMYND11*), and signaling receptor and transporter of retinol (*STRA6*).

Vascular Morphology

Microvascular architecture was analyzed via scanning electron micrographs of native lung tissue and microvascular corrosion casts using a Philips XL30 microscope (Philips, Eindhoven, the Netherlands) at 15 keV and 21 μA. Microvascular corrosion casts were generated according to a standardized protocol previously described by us.[18]

Gene Expression

RNA was isolated using the Maxwell 16 LEV RNA FFPE Purification Kit (Promega Corp.). RNA content was measured using the Qubit RNA IQ Assay (Thermo Fisher Scientific), guaranteeing a minimum of 200 ng RNA in each sample. Samples were analyzed using two commercial panels on inflammation- and kinome-specific genes (536 and 255 target genes, respectively) and the nCounter Analysis System (NanoString Technologies, Seattle, WA), which is optimized for FFPE-based experiments. Counts were normalized using the nSolver analysis software version 3.0 (NanoString Technologies). Normalization included positive normalization (geometric mean), negative normalization (arithmetic mean), and reference normalization (geometric mean). Established reference genes (glyceraldehyde-3-phosphate dehydrogenase, glucuronidase β, hypoxanthine phosphoribosyltransferase 1, phosphoglycerate kinase 1, and tubulin β class I) were designated as reference genes for standardization processes. Assembling of parameters from both panels was conducted using the nSolver software while defining a multi−reporter library file (RLF) experiment and centering on 28 genes, including expression of the reference genes that were present in both panels. Further analyses on the ascertained log2 mRNA counts were performed using R software version 3.4.4 (R Foundation for Statistical Computing, Vienna, Austria; *https://cran.r-project.org/bin/windows/base*) and the nCounter Advanced Analysis module version 1.1.5. Absolute gene expression values were analyzed and compared with those of healthy control samples. FFPE lung tissue from healthy down-sized lung transplants (ie, healthy lung tissue that was donated but not used for transplantation) was used as control. Two samples were obtained from each patient for the mRNA expression analysis. Because of technical problems, only 12 of 14 obtained ACD samples could be used for the analysis. However, as these failures occurred in samples from different patients, at least one sample repeat was included for each patient. *U*-tests were used for pairwise comparisons between groups. Kruskal-Wallis tests were used for multigroup comparisons, providing false discovery rates. Statistical analysis was concluded by correction for multiple testing (Holm Bonferroni method). False discovery rate values <0.05 were considered statistically significant.

Biological Pathways

Biological pathway analysis was performed using the comparison analysis module from the Ingenuity Pathway Analysis tool (Qiagen Inc., Venlo, the Netherlands) to complement our gene expression data by predictions on the activation/inhibition of biological functions. The relative gene expression signature of each ACD sample was compared with the median gene expression of the control samples. All significantly regulated genes (false discovery rate, <0.05) of these comparisons were used as input parameters. The analysis was performed with default settings. As described before, the Ingenuity Pathway Analysis tool calculates z scores as a quantitative confidence estimation that a biological function is either activated (positive z score) or inactivated (negative z score), as well as *P* values.[19] Significant differences in the predicted regulation of biological functions were determined via pairwise *U*-tests and multigroup Kruskal-Wallis tests. $P < 0.05$ was considered statistically significant.

Protein Expression

Paraffin sections (2 μm thick) of all groups were used for immunostaining. After deparaffinization twice with xylene for 10 minutes, rehydration was performed using the decreasing concentration of ethanol. The sections were subjected to heat-induced epitope retrieval in respective antibody buffer and stained with primary antibodies, according to the manufacturer's protocol using ZytoChem Plus HRP Polymer Kit (Zytomed Systems, Berlin, Germany) and 3, 3′-diaminobinzidine solution. The staining Eukitt mounting medium was used as an adhesive and a sealant. Images were taken after automated whole-slide imaging using the APERIO CS2 scanner (Leica Biosystems, Wetzlar, Germany) and ImageScope software version 12.3.3.5048 (Leica Biosystems). Pediatric healthy lung tissue as well as lung explants from patients diagnosed with PAH were used as controls. Appropriate markers were selected on the basis of the disease-specific mRNA profile and putatively involved biological pathways. Details about all antibodies utilized are depicted in Table 1. Immunostaining patterns of ACD samples were compared with appropriate control samples.

Results

Study Groups

Patient characteristics are shown in Supplemental Table S1. The ACD group was composed of five male and two female patients, and the median age at sampling was 1 month (interquartile range, 25/75; 0.58 to 8.5 months). Samples were obtained from four autopsies and two biopsies, and one sample was obtained from a lung explant of a patient

Table 1 Target Antibodies Used for Immunohistochemistry

Target of antibody	Product name	Host species	Pretreatment	Dilution	Manufacturer
CXCL12	SDF1 (CXCL12) Polyclonal Antibody (AP20632PU-N)	Rabbit	Sodium citrate buffer	1:200	Origene (Rockville, MD)
HIF1A	Anti—HIF-1 α antibody (ESEE122; ab8366)	Mouse	Tris-EDTA buffer	1:1000	Abcam (Cambridge, UK)
TIE2 (TEK)	Anti-TIE2, C-terminal antibody (SAB4502942)	Rabbit	Sodium citrate buffer	1:500	Sigma Aldrich (St. Louis, MO)
BMPR2	Anti-BMPR2 antibody (1F12; ab130206)	Rabbit	Sodium citrate buffer	1:5000	Abnova (Taipei, Taiwan)
WNT10b	Anti-Wnt10b antibody (ab70816)	Rabbit	Tris-EDTA buffer	1:500	Abcam
VEGFR1	Recombinant Anti-VEGF Receptor 1 antibody (Y103; ab32152)	Mouse	Tris-EDTA buffer	1:50	Abcam
STAT3	Recombinant Anti-STAT3 (phosphorylated Y705) antibody (EPR23968-52; ab267373)	Mouse	Tris-EDTA buffer	1:50	Abcam

BMPR2, bone morphogenetic protein receptor type 2; HIF1A, hypoxia-inducible factor 1α; TIE2 (TEK), TEK receptor tyrosine kinase; VEGFR1, vascular endothelial growth factor 1; WNT10b, WNT family member 10b.

who underwent lung transplantation. Pathogenic variants were not identified. The PAH group was composed of 3 male and 17 female patients, and the median age at sampling was 25.5 years (interquartile range, 25/75; 16.25 to 37.25 years). Clinical information regarding the control group is not available, to respect legal regulations and the anonymity of donors.

Morphologic Analysis

In all cases, the diagnosis of ACD/PAH was confirmed histologically by three experienced pulmonary pathologists (L.N., F.L., and D.D.J.). As shown in Figure 1, the histopathologic workup revealed typical features of ACD in all cases (ie, rarefied pulmonary capillaries, thickened alveolar septa with malapposed capillaries, medial hypertrophy of the small pulmonary arteries, and pulmonary venous dilation), whereas suspected misaligned pulmonary veins were present in $n = 4$ cases. Scanning electron microscopy of microvascular corrosion casts revealed multiple angiomatoid-like expansions of the vascular plexus with widened, deformed, blunt-ended capillaries and without functional capillary network or any perceptible vessel hierarchy. In addition, multiple intussusceptive pillars were observed in loco typico, indicating early stages of intussusceptive angiogenesis. High-magnification scanning electron microscopy of native lung tissue showed thickened alveolar septa and protrusions within the alveolar wall, as well as malapposed and flattened capillaries.

Gene Expression

As depicted in Figure 2, 163 of 791 genes showed a differential expression on the mRNA level compared with controls: $n = 96$ in ACD, and $n = 94$ in PAH. Of these, 26 genes showed similar expression in both entities: increased expression was found for activin A receptor type 2B (*ACVR2B*), ataxia telangiectasia-related serine/threonine kinase (*ATR*), aurora kinase A (*AURKA*), calcium/calmodulin-dependent protein kinase IV (*CAMK4*), casein kinase 1G3 and 2A1 (*CSNK1G3/2A1*), capped intron-containing pre-mRNA—like kinases 2 and 4 (*CLK2/4*), ephrin type-A receptor 3 (*EPHA3*), high-mobility group nucleosome-binding domain 1 (*HMGN1*), microtubule affinity regulating kinase 1 (*MARK1*), microtubule-associated serine/threonine kinases 2 and 4 (*MAST2/4*), nuclear factor of activated T cells 3 (*NFATC3*), protein kinase AMP-activated catalytic subunit α 1 (*PRKAA1*), serine/arginine-rich splicing factor protein kinase 2 (*SRPK2*), protein kinase-like protein sugen kinase 196 (*SGK196*), transforming growth factor-β regulator 4 (*TBRG4*), Tau tubulin kinase 2 (*TTBK2*), vaccinia virus B1R-related kinase 2 (*VRK2*), and several mitogen-activated protein kinases (*MAPK*), whereas decreased expression was found for G-protein—coupled receptor kinase 6 (*GRK6*) and IL-10 (*IL10*). C-X-C motif chemokine receptor 4 (*CXCR4*) showed decreased expression in ACD and increased expression in PAH. Apart from these equally regulated genes, the study focused on genes that are known to be involved in lung development, vasculogenesis, angiogenesis, and the development or progression of pulmonary hypertension. In this respect, there was increased expression of transforming growth factor-β3 (*TGFB3*), activin A receptor type 2A (*ACVR2A*), budding uninhibited by benzimidazoles 1 mitotic checkpoint serine/threonine kinase (*BUB1*), calcium/calmodulin-dependent protein kinase II delta (*CAMK2D*), cyclin-dependent kinases 1, 6, and 20 (*CDK1/6/20*), death domain—associated protein (*DAXX*),

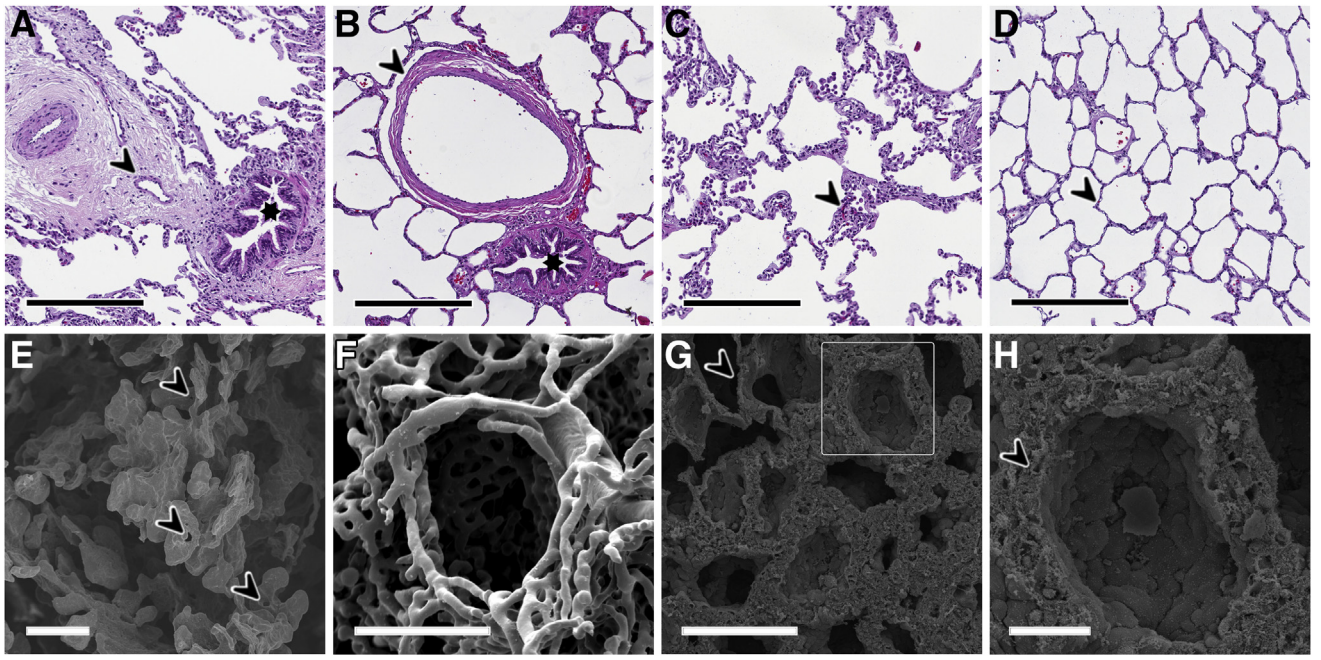

Figure 1 Morphology of alveolar capillary dysplasia with misalignment of the pulmonary veins (ACD/MPV). **A** and **C:** Histopathologic morphology of ACD/MPV. **B** and **D:** Healthy control tissue from a 5-year—old child. **A:** Typical misalignment of the pulmonary veins (**arrowhead**) within the bronchiovascular bundle adjacent to a bronchiole (**asterisk**) and a media-hypertrophied pulmonary artery branch. **B:** Physiological bronchiovascular bundle composed of a bronchiole (**asterisk**) and pulmonary artery branch (**arrowhead**). **C:** Immature lung tissue with unapposed alveolar capillaries within widened alveolar septa (**arrowhead**), as well as small clusters of macrophages in the alveolar spaces. **D:** In contrast, physiological thin-walled alveolar septa with well-aligned capillaries (**arrowhead**). **E:** Scanning electron micrograph of a microvascular corrosion cast, showing distinctive angiomatoid-like expansions of the vascular plexus in alveolar capillary dysplasia, characterized by widened, deformed, blunt-ended capillaries. Neither a functional capillary network nor a perceptible vessel hierarchy was observed. However, there was a multitude of typically localized intussusceptive pillars (**arrowheads**), indicating early stages of intussusceptive angiogenesis. **F:** Physiological thin-walled alveolar capillary network of healthy lung tissue for comparison purposes. **G:** Native scanning electron micrograph, showing juxtapositioned normally dimensioned (**arrowhead**) and thickened alveolar structures. **H: Inset** of **G**, showing one alveolus with thickened alveolar septa, protrusions within the alveolar wall, and multiple malapposed, flattened capillaries (**arrowhead**). Scale bars: 300 μm (**A**—**D**); 200 μm (**E** and **G**); 100 μm (**F**); 50 μm (**H**).

glycogen synthase kinase 3β (*GSK3B*), homeodomain-interacting protein kinase 3 (*HIPK3*), integrin-linked kinase (*ILK*), protein tyrosine kinase 7 (*PTK7*), receptor tyrosine kinase-like orphan receptor 2 (*ROR2*), transcription factor 4 (*TCF4*), nuclear factor of activated T cells 3 (*NFATC3*), and thymic stromal lymphopoietin (*TSLP*), as well as a decreased expression of arachidonate 5-lipoxygenase (*ALOX5*), CD163 (*CD163*), cyclin-dependent kinase 5 (*CDK5*), colony-stimulating factor 3 (*CSF3*), *CXCL2/9*, C-X-C motif chemokine receptor 1 (*CXCR1*), feline Gardner-Rasheed sarcoma viral oncogene homolog proto-oncogene, Src family tyrosine kinase (*FGR*), IL-6 (*IL6*), IL-18 receptor accessory protein (*IL18RAP*), matrix metalloproteinase 9 (*MMP9*), prostaglandin E receptor 1 and 4 (*PTGER1/4*), ras homolog family member A (*RHOA*), as well as toll-like receptors 2 and 4 (*TLR2/4*).

Biological Pathways

Biological pathway analysis revealed several activated or inhibited molecular pathways in ACD and PAH, as shown in Supplemental Table S2. In comparison to healthy controls, increased activity was observed for angiopoietin, CXCR4 signaling, hypoxia-inducible factor 1α (HIF1A) signaling, transforming growth factor-β (TGFB) signaling, bone morphogenetic protein (BMP) signaling, vascular endothelial growth factor (VEGF) signaling, STAT3 signaling, NF-κB signaling, mechanistic target of rapamycin kinase signaling, and cardiac hypertrophy signaling pathways in both diseases. TLR signaling, acute-phase response signaling, and IL-6 signaling showed lower activity in ACD but higher activity in PAH.

Protein Expression

On the basis of the disease-specific mRNA expression, the results of the biological pathway analysis and the morphologic findings of an increased prevalence of intussusceptive angiogenesis, we selected TEK receptor tyrosine kinase (TIE2), CXCL12, HIF1A, bone morphogenetic protein receptor 2 (BMPR2), Wnt family member 10b (Wnt10b), STAT3, and VEGF receptor 1 (VEGFR1) as target molecules. The results of the immunohistochemical staining are depicted in Figures 3 and 4.

As suggested, markers of intussusceptive angiogenesis, CXCL12, HIF1A, and TIE2 showed a striking positivity in ACD. Particularly, there was a striking positivity for TIE2 in almost all macrophages in ACD. In comparison, all macrophages found in PAH lungs appeared $TIE2^{-}$, and only a few

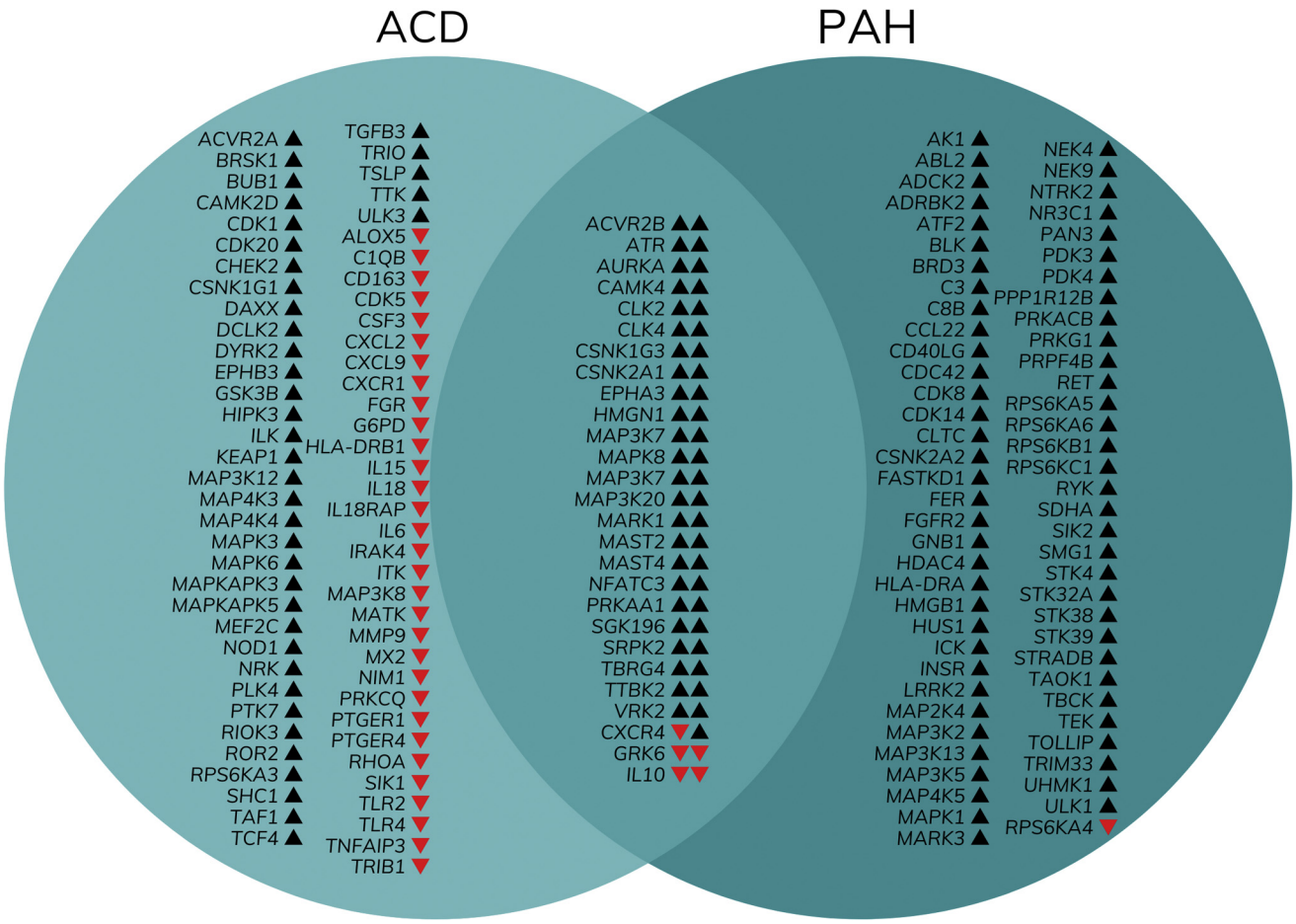

Figure 2 Venn diagram of differentially regulated genes in alveolar capillary dysplasia (ACD) and pulmonary arterial hypertension (PAH). **Arrowheads** indicate increased (**black arrowheads**) or decreased (**red arrowheads**) activity of the respective genes in each group; in the overlapping area (middle), **left** and **right arrowheads** indicate the expression in ACD and PAH, respectively.

(approximately 10%) were $TIE2^{+}$ in healthy controls. CXCL12 and HIF1A were found predominantly in endothelial cells, respiratory epithelial cells, and septa, as well as in bronchus-associated lymphoid tissue. PAH lungs appeared $CXCL12^{-}$ and only slightly $HIF1A^{+}$, whereas both markers were enhanced in respiratory epithelial cells of healthy controls. This was also the case for endothelial cells and alveolar type II cells; however, this was less pronounced compared with ACD lungs.

Regarding the markers of biological pathways that showed increased activity on the mRNA level, immunostaining revealed strong cytoplasmic positivity for BMPR2, Wnt10b, and VEGFR1, as well as a distinct nuclear positivity for STAT3 in respiratory epithelial cells and bronchus-associated lymphoid tissue. In addition, endothelial cells showed a slight positivity for BMPR2, Wnt10b, and VEGFR1. In comparison, STAT3 was barely found in PAH lungs and solely in respiratory epithelial cells of controls, whereas BMPR2 was found in the same structures as in ACD, but less powerful. Wnt10b, as well as VEGFR1, showed a comparable specificity and intensity in ACD, PAH, and controls.

Discussion

ACD is an extremely rare but severe and incurable lung developmental disorder that is fatal without a lung transplant. Because it manifests in the first days of life, a quick diagnosis is essential. Because the diagnosis can only be confirmed genetically in about half of cases, and genetic testing takes days to weeks, it has limited applicability in clinical practice for immediate therapeutic decisions. Histologic diagnosis is also often challenging or inconclusive. This work was able to show, for the first time, that ACD not only differs from other forms of PAH in conventional microscopy, but also shows considerable differences at the RNA and protein level, which may also be helpful for diagnostic purposes. Thus, the current results help to better understand the complex pathophysiology of ACD. In addition, the study demonstrated an angiomatoid-like expansion of the vascular plexus and a high prevalence of intussusceptive angiogenesis in ACD, suggesting the elucidation of specific angiogenesis inhibitors in this disease.

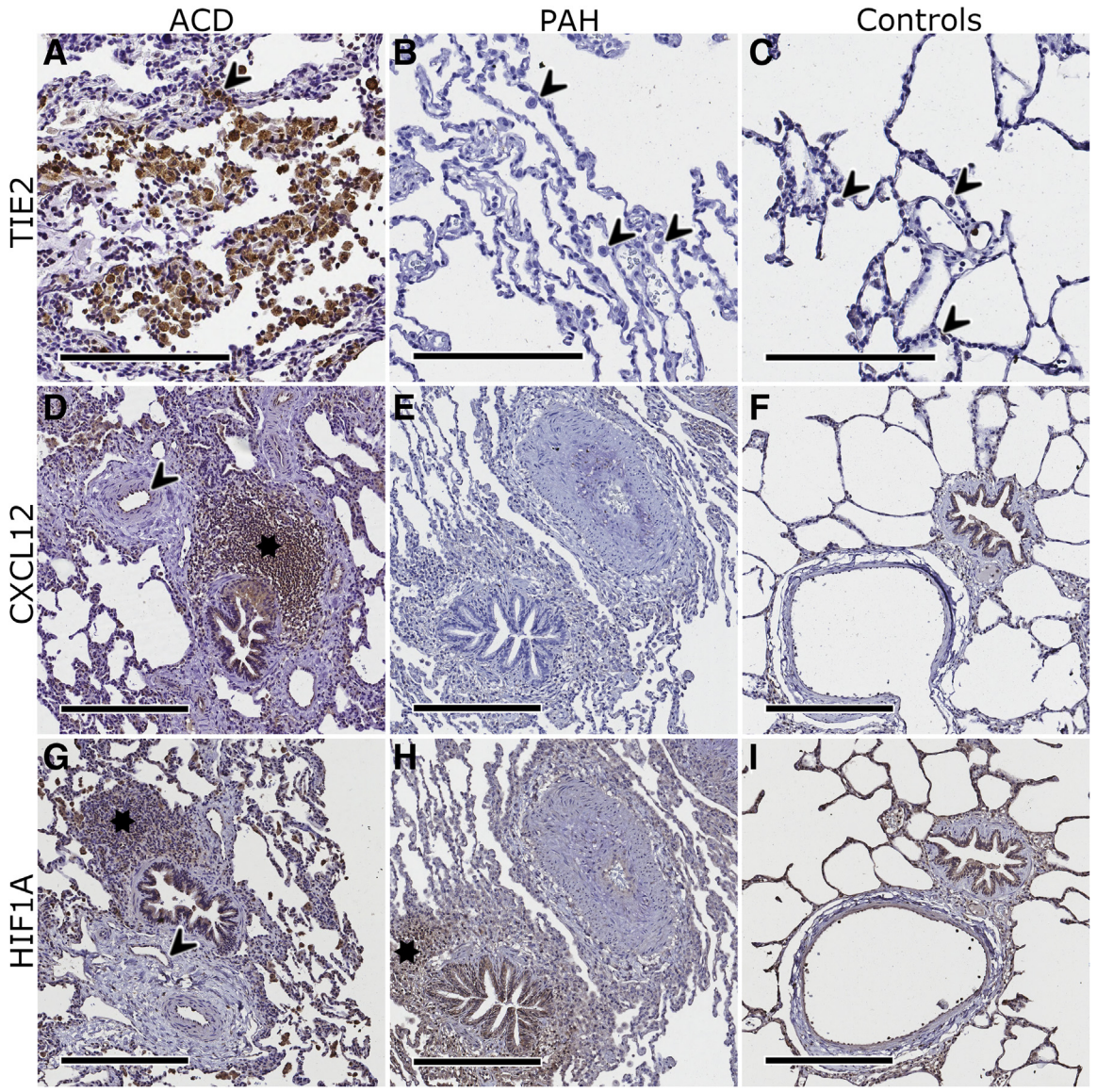

Figure 3 Immunostaining with established markers of intussusceptive angiogenesis in alveolar capillary dysplasia (ACD) with misalignment of the pulmonary veins, idiopathic pulmonary arterial hypertension (PAH), and pediatric healthy controls. **A:** Large clusters of macrophages within the alveolar spaces as well as migrating macrophages within the alveolar septa (**arrowhead**) were observed in ACD samples. All macrophages showed a consistent positivity for TEK receptor tyrosine kinase (TIE2). **B** and **C:** In contrast, in PAH lungs (**B**), all macrophages appeared $TIE2^{-}$ (**arrowheads**); and in controls (**C**), only few scattered $TIE2^{+}$ macrophages were found between predominantly $TIE2^{-}$ macrophages (**arrowheads**). **D** and **G:** CXCL12 (**D**) and hypoxia-inducible factor 1α (HIF1A; **G**) showed a cytoplasmic enrichment in endothelial cells (**arrowhead**), respiratory epithelial cells, and septa, as well as in bronchus-associated lymphoid tissue (BALT; **asterisk**) in ACD lungs. **E**, **F**, **H**, and **I:** In PAH lungs, CXCL12 (**E**) was negative, whereas HIF1A (**H**) was enhanced, predominantly in bronchial epithelial cells, and BALT (**asterisk**); and in healthy controls, CXCL12 (**F**) was found solely in respiratory epithelial cells and HIF1A (**I**) in respiratory epithelial cells and alveolar type II cells, as well as slightly in endothelial cells. Scale bars: 200 μm (**A**–**C**); 300 μm (**D**–**I**).

The formation of new blood vessels is due to vasculogenesis, *de novo* formation of blood vessels from angioblastic precursor cells during early stages of embryonic development,[20] as well as angiogenesis, which is characterized by vascular neoformation from preexisting vessels and occurs during the entire life of an organism.[21] In classic sprouting angiogenesis, small vessel sprouts grow out of existing blood vessels toward higher concentrations of vascular growth factors, such as VEGF (eg, in the context of wound healing or tumor angiogenesis).[22] In contrast, intussusceptive angiogenesis (also referred to as splitting angiogenesis) is another, more recently described type of blood vessel neoformation, occurring due to the splitting of an existing blood vessel into two new lumens within minutes to hours.[23,24] Recent studies revealed an association of distinct molecular markers and signaling pathways as well as selected subtypes of macrophages with the induction and progression of intussusceptive angiogenesis. Recently, angiopoietin signaling, HIF1A signaling, and CXCR4 signaling emerged as key players in this context.[25,26]

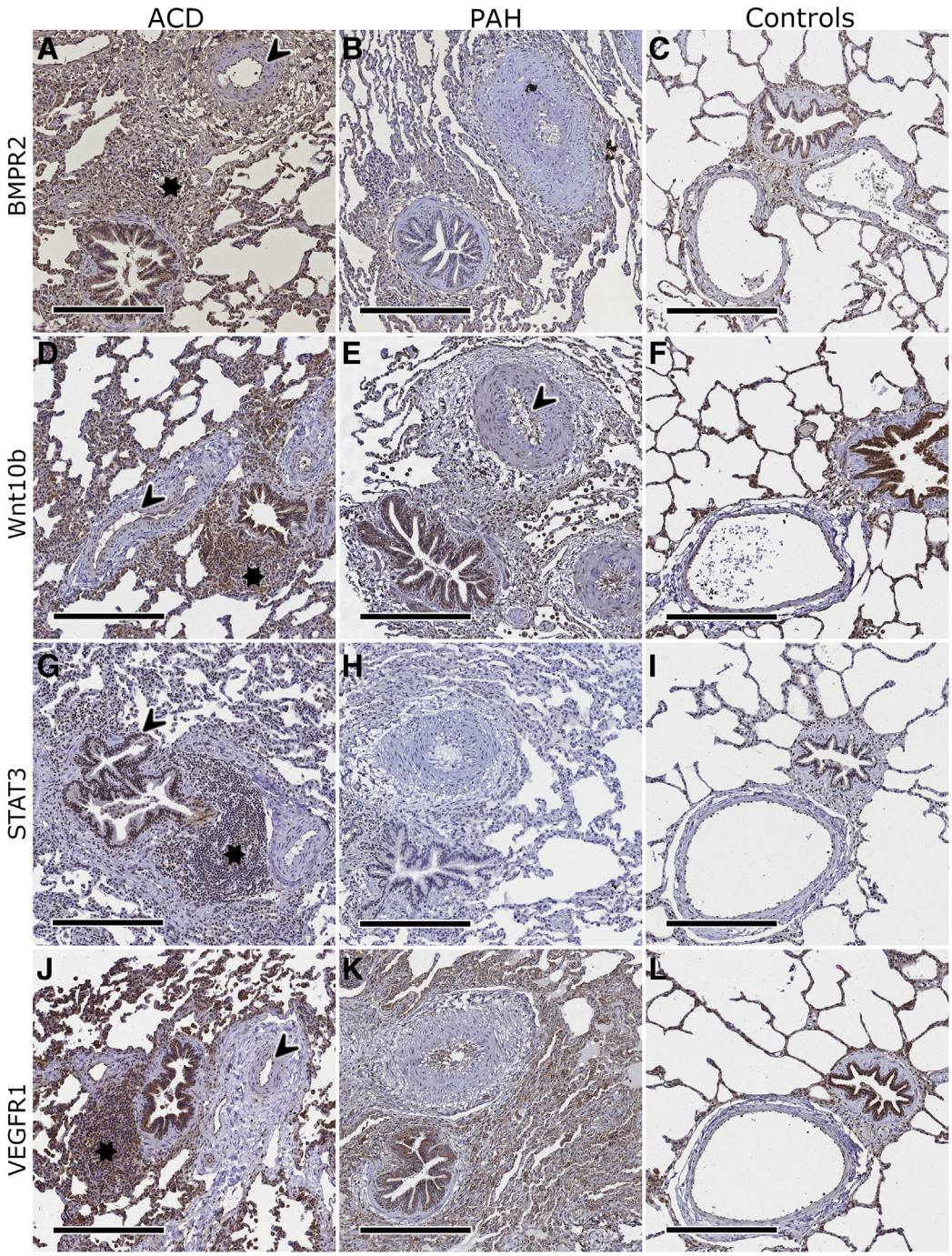

Figure 4 Immunostaining with markers based on the disease-specific mRNA profile in alveolar capillary dysplasia (ACD) with misalignment of the pulmonary veins, idiopathic pulmonary arterial hypertension (PAH), and pediatric healthy controls. **A:** In ACD, bone morphogenetic protein receptor type 2 (BMPR2) showed a powerful staining of bronchial epithelial cells and bronchus-associated lymphoid tissue (**asterisk**), as well as a specific enhancement in endothelial cells (**arrowhead**). **B** and **C:** In PAH (**B**) as well as in healthy controls (**C**), BMPR2 was slightly positive in respiratory epithelial cells and alveolar type II cells; however, the staining intensity appeared much lower, as in ACD. **D:** In ACD, Wnt family member 10b (Wnt10b) was strongly positive predominantly in macrophages, respiratory epithelial cells, alveolar type II cells, and bronchus-associated lymphoid tissue (**asterisk**), as well as slightly in endothelial cells (**arrowhead**). **E** and **F:** In PAH lungs (**E**) as well as in healthy controls (**F**), Wnt10b showed a comparable specificity and staining intensity, despite the observation that in PAH lungs, not endothelial cells but sclerotic structures of obliterated pulmonary artery branches (**arrowhead**) were stained. **G:** In ACD, STAT3 showed a nuclear enhancement predominantly in respiratory epithelial cells (**arrowhead**), scattered intraseptal lymphocytes, and bronchus-associated lymphoid tissue (BALT; **asterisk**). **H** and **I:** In contrast, no positive structures were found in PAH (**H**) and only a slight nuclear positivity in scattered lymphocytes and bronchial epithelial cells in controls (**I**). **J:** In ACD, vascular endothelial growth factor receptor 1 (VEGFR1) showed a strong staining of respiratory epithelial cells, BALT (**asterisk**), and macrophages as well as a slight enhancement in endothelial cells (**arrowhead**). **K** and **L:** In PAH (**K**) as well as in controls (**L**), VEGFR1 was enriched in the same structures as in ACD, except for endothelial cells; however, because of the significantly lower magnitude of macrophages and lymphatic tissue, the amount of positive structures was markedly lower. Scale bar = 300 μm (**A**–**L**).

CXCR4 is a transmembrane G-protein–coupled receptor, frequently expressed in tumors, promoting tumor-associated angiogenesis together with its ligand, CXCL12. In addition, $TIE2^+$ macrophages have been suspected to participate in the formation of intussusceptive pillars (C.W., unpublished data). Hence, the current study focused on these markers and found many congruities: i) the increased activity of HIF1A and CXCR4 signaling as well as the strong positivity of endothelial and epithelial structures for HIF1A and the CXCR4-ligand CXCL12; ii) the large number of $TIE2^+$ macrophages migrating from the alveolar capillary vessels through the thickened alveolar septa and eventually clustering in the alveolar spaces; and iii) the up-regulation of the angiopoietin signaling pathway, which is crucial for attracting $TIE2^+$ macrophages. We hypothesize that $TIE2^+$ macrophages encountering the endothelial surface induce a release of chemoattractants, which increase activity of CXCR4 and angiopoietin signaling, leading to loosening up of endothelial surface structures and consequently to intussusceptive pillar formation, as the origin of intussusceptive angiogenesis, visualized in Figure 5.

Endothelial cells are considered as genetically stable and therefore less susceptible for the development of multidrug resistance. In addition, endothelial cells are available intravenously. These properties facilitate the use of endothelial cells as potential therapeutic targets. Endothelial cells grow toward higher concentrations of VEGF conditioned by the expression of active VEGFR on their surface. This molecular interplay is targeted by specific anti-angiogenic agents, predominantly in the treatment of several cancer entities. Most agents currently in use, or in clinical testing, target the VEGF/VEGFR axis (eg, bevacizumab, vatalanib, sorafenib, and regorafenib). Of these, regorafenib is interesting in the context of ACD as it targets several kinases beyond VEGF/VEGFR, including TIE2.[27] Given that $TIE2^+$ macrophages appear to play an important role for intussusceptive angiogenesis, it appears logical to test the effect of regorafenib on the aberrative vascular plexus in ACD in future studies.

Beyond those pathways thought to be relevant in intussusceptive angiogenesis, this study found an increased expression of several genes associated with the TGFB and BMP signaling pathways. TGFB signaling is involved in several biological functions, such as immune suppression, angiogenesis, wound healing, and epithelial-to-mesenchymal transition.[28] Moreover, it is a well-known driver of PAH development,[29] and selective blockage of its subunits TGF-β1 and TGF-β3 is effective in attenuating PAH and preventing pulmonary vascular remodeling in multiple animal models.[30] One essential mediator of TGFB signaling and TGFB receptor formation is the serine/threonine kinase BUB1.[28] BMPR2 is a member of the TGFB superfamily, and its subtypes are encoded by ACVR2A and ACVR2B. BMPR2 mediates the functions of activins, and dysfunctional variants of this gene are involved in several biological processes leading to PAH. Physiologically, BMPR2 inhibits the proliferation of vascular smooth muscle cells and promotes the survival of pulmonary arterial endothelial cells. Therefore, BMPR prevents tissue damage and concomitant inflammatory responses. In addition, BMPR2 is one of the major predictors of hereditary PAH.[31] The current study indicated an increased expression of TGFB3, ACVR2A/B, and BUB1 at the mRNA level as well as increased expression of BMPR2 at the protein level in ACD compared with PAH and healthy controls. However, there were also some genes with a decreased mRNA expression signature that play a role in TGFB signaling (ie, *ALOX5*, *RHOA*, and *CSF3*). *ALOX5* encodes a member of the lipoxygenase family that is required for the synthesis of leukotrienes from arachidonic acid. *ALOX5* is well characterized as a potential hypoxia-induced mediator of PAH development, whereas its metabolites promote pulmonary vasoconstriction and endothelial cell proliferation.[32] *RHOA* is a small TGFB-induced GTPase protein that is involved in several biological functions, such as cytoskeleton regulation, and it has been suggested as a promoter of PAH development.[33] Hence, the relevance of decreased *ALOX5* and *RHOA* expression in ACD/MPV remains unclear. However, the increased BMP signaling activity might be an

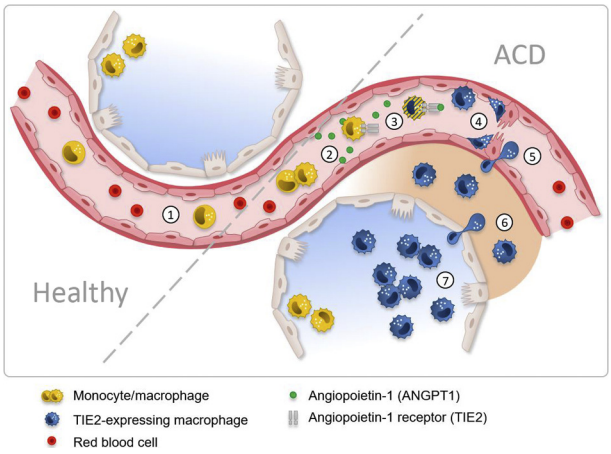

Figure 5 This figure illustrates the hypothesis of the induction of intussusceptive pillar formation in the context of alveolar capillary dysplasia (ACD). As can be seen in (**1**), there is a coexistence of physiological alveolar regions, characterized by thin septa and a short gas exchange way, maldeveloped regions with thickened alveolar septa, and a highly extended way from the air spaces to the alveolar capillaries. (**2**) The impaired gas exchange in affected regions results in tissue hypoxia and concomitant activation of hypoxia-associated signaling pathways, such as hypoxia-inducible factor 1α, C-X-C motif chemokine receptor 4, and angiopoietin signaling, as well as increased expression of angiopoietin-1 (ANGPT1) in endothelial cells. (**3**) ANGPT1 molecules on endothelial cells bind to TEK receptor tyrosine kinase (TIE2) receptors expressed on circulating macrophages and therefore initiate (**4**) the adhesion of $TIE2^+$ macrophages to the endothelial surface. (**5**) These macrophages migrate through the thickened septa (**6**) and accumulate in the alveolar spaces (**7**). Thereby, the contact between $TIE2^+$ macrophages and the endothelial cells might induce a loosening of the endothelial surface, and a movement toward the opposite endothelial surface, resulting in an intussusceptive pillar formation. Subsequently, circulating blood-borne angiogenic progenitor cells might be integrated within this pillar and promote the septum formation, resulting in the division of an existing vessel into two new lumens.

attempt by the endothelial cells to face the increased pulmonary vascular resistance, as well as the resulting pulmonary hypertension. *CSF3* is a TGFB-induced protein-regulated gene that enhances nitric oxide production in pulmonary endothelial cells. Liu et al[34] have identified TGFB-induced protein as a developmentally regulated protein that promotes NF-κB–mediated angiogenesis during early alveolarization via *CSF3*-mediated enhancing of nitric oxide production. Consequently, dysregulation of *CSF3* impairs alveolar and vascular growth. In summary, these results suggest an important role of TGFB and particularly BMP signaling in the development of ACD. However, these alterations might also be a consequence of hypoxia and consecutive tissue damage, rather than causative for ACD.

The *STAT3* gene is a transcription factor involved in several biological functions, such as cell growth and apoptosis via mediation of a variety of genes. It is phosphorylated by receptor-associated Janus kinases in response to several cytokines and growth factors.[35] HIPK3 is an important STAT3-associated regulator of cell function and vessel growth. It encodes a circular RNA that in turn promotes proliferation, migration, and angiogenesis in human pulmonary artery endothelial cells by regulating the miR-328-3p/STAT3 axis.[36] This study found increased activity of STAT3 signaling in ACD, corresponding with a significantly increased expression of STAT3 at the protein level in ACD, compared with PAH and healthy controls. Thus, STAT3 signaling might contribute to the massive expansion of the vascular plexus in ACD, which was demonstrated in the corrosion casts.

The canonical Wnt signaling pathway represents an important, highly conserved signal transduction pathway involved in several embryonic processes, including cell proliferation, migration, behavior, and polarity, as well as cell fate specification.[37,38] PTK7 is a Wnt downstream molecule involved in embryogenesis and angiogenesis,[39] and its mRNA levels are modulated via VEGF.[40] ROR2 is a receptor tyrosine kinase that mediates Wnt5 signaling, which is crucial for physiological lung morphogenesis, whereas dysregulation of Wnt5 has been shown to cause misdirected airway and vascular tubulogenesis (ie, abnormal branching of distal airways as well as defects in capillaries and alveolar airspaces). TCF4 serves as a binding partner for broad-complex, tramtrack and bric a brac domain and Carney complex homolog 1, and their binding results in blockage of Wnt-targeted promoter activity and VEGF gene expression.[41] This study demonstrated increased expression of PTK7, ROR2, and TCF4, suggesting a prominent role of Wnt and VEGF signaling in the pathophysiology of ACD/MPV. However, these findings could not be corroborated at the protein level as Wnt10b and VEGFR1 showed the same expression level and specificity in ACD, PAH, and healthy control lungs. Given that ACD is caused by developmental processes that manifest during the embryonal and fetal period, gene and protein expression are in part the results of misguided pulmonary vascular development and increased pulmonary vascular resistance, and only partially reflect the initial pathologic onset of the disease.

In summary, the current study provided new insights into the capillary morphology and the gene expression of ACD. It showed a high prevalence of intussusceptive angiogenesis and a corresponding regulation of potentially contributing molecular pathways, such as CXCR4 and angiopoietin signaling, as well as a high prevalence of $TIE2^{+}$ macrophages as potential inductors of intussusceptive pillar formation. This indicates that the increased activity of STAT3 and BMP signaling likely promotes aberrant angiogenesis in this context.

The current study has some limitations, including the comparatively small sample sizes. Also, the samples used for gene expression analyses could not be prepared in a compartment-specific manner and therefore included miscellaneous tissue structures. However, this was due to limited sample sizes as most specimens were obtained from small biopsies or autopsies. However, statistical analysis showed that both the highly preserved biopsy samples, as well as the autopsy samples, showed clear and comparable molecular patterns. Therefore, degradation by autolysis was interpreted as limited.

Future studies are needed to further explore the three-dimensional and functional morphology of the pulmonary vasculature in ACD, as well as the causative pathomechanisms and potential treatment options apart from lung transplantation for this rare and fatal disease. To this end, functional testing of regorafenib will be a promising first step in the right direction.

Acknowledgments

We thank Kerstin Bahr, Annette Müller-Brechlin, Christina Petzold Muegge, Regina Engelhardt, Nicole Krönke, Edwin Lennart Busch, Caja Boekhoff, and Lennart Brandt for excellent technical support; and Nikki Chapman and Claudia Davenport for editing the article.

Author Contributions

J.C.K., L.N., M.M.H., M.P.K., and D.D.J. conceived and designed the study; J.C.K., L.N., H.S., A.K.B., G.S., M.P.K., and D.D.J. prepared materials and collected and analyzed data; J.C.K. and E.P. visualized the figures; J.C.K., L.N., M.P.K., and D.D.J. wrote the first draft of the manuscript; and all authors commented on previous versions of the manuscript. All authors read and approved the final manuscript.

Supplemental Data

Supplemental material for this article can be found at *http://doi.org/10.1016/j.ajpath.2022.05.004*.

References

1. van Loon RL, Roofthooft MT, Hillege HL, ten Harkel AD, van Osch-Gevers M, Delhaas T, Kapusta L, Strengers JL, Rammeloo L, Clur SA, Mulder BJ, Berger RM: Pediatric pulmonary hypertension in the Netherlands: epidemiology and characterization during the period 1991 to 2005. Circulation 2011, 124:1755−1764
2. Roth W, Bucsenez D, Bläker H, Berger I, Schnabel PA: Misalignment of pulmonary vessels with alveolar capillary dysplasia: association with atrioventricular septal defect and quadricuspid pulmonary valve. Virchows Arch 2006, 448:375−378
3. Martinho S, Adão R, Leite-Moreira AF, Brás-Silva C: Persistent pulmonary hypertension of the newborn: pathophysiological mechanisms and novel therapeutic approaches. Front Pediatr 2020, 8:342
4. Cater G, Thibeault DW, Beatty EC Jr, Kilbride HW, Huntrakoon M: Misalignment of lung vessels and alveolar capillary dysplasia: a cause of persistent pulmonary hypertension. J Pediatr 1989, 114:293−300
5. Deutsch GH, Young LR, Deterding RR, Fan LL, Dell SD, Bean JA, Brody AS, Nogee LM, Trapnell BC, Langston C; Pathology Cooperative Group, Albright EA, Askin FB, Baker P, Chou PM, Cool CM, Coventry SC, Cutz E, Davis MM, Dishop MK, Galambos C, Patterson K, Travis WD, Wert SE, White FV; ChILD Research Cooperative: Diffuse lung disease in young children: application of a novel classification scheme. Am J Respir Crit Care Med 2007, 176:1120−1128
6. Michalsky MP, Arca MJ, Groenman F, Hammond S, Tibboel D, Caniano DA: Alveolar capillary dysplasia: a logical approach to a fatal disease. J Pediatr Surg 2005, 40:1100−1105
7. Ito Y, Akimoto T, Cho K, Yamada M, Tanino M, Dobata T, Kitaichi M, Kumaki S, Kinugawa Y: A late presenter and long-term survivor of alveolar capillary dysplasia with misalignment of the pulmonary veins. Eur J Pediatr 2015, 174:1123−1126
8. Kodama Y, Tao K, Ishida F, Kawakami T, Tsuchiya K, Ishida K, Takemura T, Nakazawa A, Matsuoka K, Yoda H: Long survival of congenital alveolar capillary dysplasia patient with NO inhalation and epoprostenol: effect of sildenafil, beraprost and bosentan. Pediatr Int 2012, 54:923−926
9. Towe CT, White FV, Grady RM, Sweet SC, Eghtesady P, Wegner DJ, Sen P, Szafranski P, Stankiewicz P, Hamvas A, Cole FS, Wambach JA: Infants with atypical presentations of alveolar capillary dysplasia with misalignment of the pulmonary veins who underwent bilateral lung transplantation. J Pediatr 2018, 194:158−164.e1
10. Nakajima D, Oda H, Mineura K, Goto T, Kato I, Baba S, Ikeda T, Chen-Yoshikawa TF, Date H: Living-donor single-lobe lung transplantation for pulmonary hypertension due to alveolar capillary dysplasia with misalignment of pulmonary veins. Am J Transplant 2020, 20:1739−1743
11. Stankiewicz P, Sen P, Bhatt SS, Storer M, Xia Z, Bejjani BA, et al: Genomic and genic deletions of the FOX gene cluster on 16q24.1 and inactivating mutations of FOXF1 cause alveolar capillary dysplasia and other malformations. Am J Hum Genet 2009, 84:780−791
12. Szafranski P, Gambin T, Dharmadhikari AV, Akdemir KC, Jhangiani SN, Schuette J, et al: Pathogenetics of alveolar capillary dysplasia with misalignment of pulmonary veins. Hum Genet 2016, 135:569−586
13. Edwards JJ, Murali C, Pogoriler J, Frank DB, Handler SS, Deardorff MA, Hopper RK: Histopathologic and genetic features of alveolar capillary dysplasia with atypical late presentation and prolonged survival. J Pediatr 2019, 210:214−219.e2
14. Pucci A, Zanini C, Ferrero F, Arisio R, Valori A, Abbruzzese P, Forni M: Misalignment of lung vessels: diagnostic role of conventional histology and immunohistochemistry. Virchows Arch 2003, 442:597−600
15. Miranda J, Rocha G, Soares H, Vilan A, Brandão O, Guimarães H: Alveolar capillary dysplasia with misalignment of pulmonary veins (ACD/MPV): a case series. Case Rep Crit Care 2013, 2013:327250
16. Norvik C, Westöö CK, Peruzzi N, Lovric G, van der Have O, Mokso R, Jeremiasen I, Brunnström H, Galambos C, Bech M, Tran-Lundmark K: Synchrotron-based phase-contrast micro-CT as a tool for understanding pulmonary vascular pathobiology and the 3-D microanatomy of alveolar capillary dysplasia. Am J Physiol Lung Cell Mol Physiol 2020, 318:L65−L75
17. Ackermann M, Tafforeau P, Wagner WL, Walsh CL, Werlein C, Kühnel MP, Länger FP, Disney C, Bodey AJ, Bellier A, Verleden SE, Lee PD, Mentzer SJ, Jonigk DD: The bronchial circulation in COVID-19 pneumonia. Am J Respir Crit Care Med 2022, 205:121−125
18. Ackermann M, Houdek JP, Gibney BC, Ysasi A, Wagner W, Belle J, Schittny JC, Enzmann F, Tsuda A, Mentzer SJ, Konerding MA: Sprouting and intussusceptive angiogenesis in postpneumonectomy lung growth: mechanisms of alveolar neovascularization. Angiogenesis 2014, 17:541−551
19. Neubert L, Borchert P, Stark H, Hoefer A, Vogel-Claussen J, Warnecke G, Eubel H, Kuenzler P, Kreipe HH, Hoeper MM, Kuehnel M, Jonigk D: Molecular profiling of vascular remodeling in chronic pulmonary disease. Am J Pathol 2020, 190:1382−1396
20. Galambos C, deMello DE: Molecular mechanisms of pulmonary vascular development. Pediatr Dev Pathol 2007, 10:1−17
21. Djonov V, Schmid M, Tschanz SA, Burri PH: Intussusceptive angiogenesis: its role in embryonic vascular network formation. Circ Res 2000, 86:286−292
22. Vega R, Carretero M, Travasso RDM, Bonilla LL: Notch signaling and taxis mechanisms regulate early stage angiogenesis: a mathematical and computational model. PLoS Comput Biol 2020, 16:e1006919
23. Ackermann M, Stark H, Neubert L, Schubert S, Borchert P, Linz F, Wagner WL, Stiller W, Wielpütz M, Hoefer A, Haverich A, Mentzer SJ, Shah HR, Welte T, Kuehnel M, Jonigk D: Morphomolecular motifs of pulmonary neoangiogenesis in interstitial lung diseases. Eur Respir J 2020, 55:1900933
24. Mentzer SJ, Konerding MA: Intussusceptive angiogenesis: expansion and remodeling of microvascular networks. Angiogenesis 2014, 17:499−509
25. Ali Z, Mukwaya A, Biesemeier A, Ntzouni M, Ramsköld D, Giatrellis S, Mammadzada P, Cao R, Lennikov A, Marass M, Gerri C, Hildesjö C, Taylor M, Deng Q, Peebo B, Del Peso L, Kvanta A, Sandberg R, Schraermeyer U, Andre H, Steffensen JF, Lagali N, Cao Y, Kele J, Jensen LD: Intussusceptive vascular remodeling precedes pathological neovascularization. Arterioscler Thromb Vasc Biol 2019, 39:1402−1418
26. Dimova I, Karthik S, Makanya A, Hlushchuk R, Semela D, Volarevic V, Djonov V: SDF-1/CXCR4 signalling is involved in blood vessel growth and remodelling by intussusception. J Cell Mol Med 2019, 23:3916−3926
27. Ettrich TJ, Seufferlein T: Regorafenib. Recent Results Cancer Res 2018, 211:45−56
28. Nyati S, Schinske-Sebolt K, Pitchiaya S, Chekhovskiy K, Chator A, Chaudhry N, Dosch J, Van Dort ME, Varambally S, Kumar-Sinha C, Nyati MK, Ray D, Walter NG, Yu H, Ross BD, Rehemtulla A: The kinase activity of the Ser/Thr kinase BUB1 promotes TGF-β signaling. Sci Signal 2015, 8:ra1
29. de la Cuesta F, Passalacqua I, Rodor J, Bhushan R, Denby L, Baker AH: Extracellular vesicle cross-talk between pulmonary artery smooth muscle cells and endothelium during excessive TGF-β signalling: implications for PAH vascular remodelling. Cell Commun Signal 2019, 17:143
30. Yung LM, Nikolic I, Paskin-Flerlage SD, Pearsall RS, Kumar R, Yu PB: A selective transforming growth factor-β ligand trap attenuates pulmonary hypertension. Am J Respir Crit Care Med 2016, 194:1140−1151
31. Montani D, Girerd B, Jaïs X, Laveneziana P, Lau EMT, Bouchachi A, Hascoët S, Günther S, Godinas L, Parent F, Guignabert C, Beurnier A, Chemla D, Hervé P, Eyries M, Soubrier F, Simonneau G, Sitbon O, Savale L, Humbert M: Screening for

pulmonary arterial hypertension in adults carrying a BMPR2 mutation. Eur Respir J 2021, 58:2004229
32. Porter KM, Kang BY, Adesina SE, Murphy TC, Hart CM, Sutliff RL: Chronic hypoxia promotes pulmonary artery endothelial cell proliferation through H2O2-induced 5-lipoxygenase. PLoS One 2014, 9:e98532
33. Zhang Y, Yuan RX, Bao D: TGF-β1 promotes pulmonary arterial hypertension in rats via activating RhoA/ROCK signaling pathway. Eur Rev Med Pharmacol Sci 2020, 24:4988−4996
34. Liu M, Iosef C, Rao S, Domingo-Gonzalez R, Fu S, Snider P, Conway SJ, Umbach GS, Heilshorn SC, Dewi RE, Dahl MJ, Null DM, Albertine KH, Alvira CM: Transforming growth factor-induced protein promotes NF-κB-mediated angiogenesis during postnatal lung development. Am J Respir Cell Mol Biol 2021, 64: 318−330
35. Hillmer EJ, Zhang H, Li HS, Watowich SS: STAT3 signaling in immunity. Cytokine Growth Factor Rev 2016, 31:1−15
36. Hong L, Ma X, Liu J, Luo Y, Lin J, Shen Y, Zhang L: Circular RNA-HIPK3 regulates human pulmonary artery endothelial cells function and vessel growth by regulating microRNA-328-3p/STAT3 axis. Pulm Circ 2021, 11:20458940211000234
37. Clevers H, Nusse R: Wnt/β-catenin signaling and disease. Cell 2012, 149:1192−1205
38. Taciak B, Pruszynska I, Kiraga L, Bialasek M, Krol M: Wnt signaling pathway in development and cancer. J Physiol Pharmacol 2018, 69: 185−196
39. Shin WS, Na HW, Lee ST: Biphasic effect of PTK7 on KDR activity in endothelial cells and angiogenesis. Biochim Biophys Acta 2015, 1853:2251−2260
40. Shin WS, Maeng YS, Jung JW, Min JK, Kwon YG, Lee ST: Soluble PTK7 inhibits tube formation, migration, and invasion of endothelial cells and angiogenesis. Biochem Biophys Res Commun 2008, 371: 793−798
41. Jiang L, Jia M, Wei X, Guo J, Hao S, Mei A, Zhi X, Wang X, Li Q, Jin J, Zhang J, Li S, Meng D: Bach1-induced suppression of angiogenesis is dependent on the BTB domain. EBioMedicine 2020, 51: 102617